Supplemental material

Li et al., https://doi.org/10.1084/jem.20171934

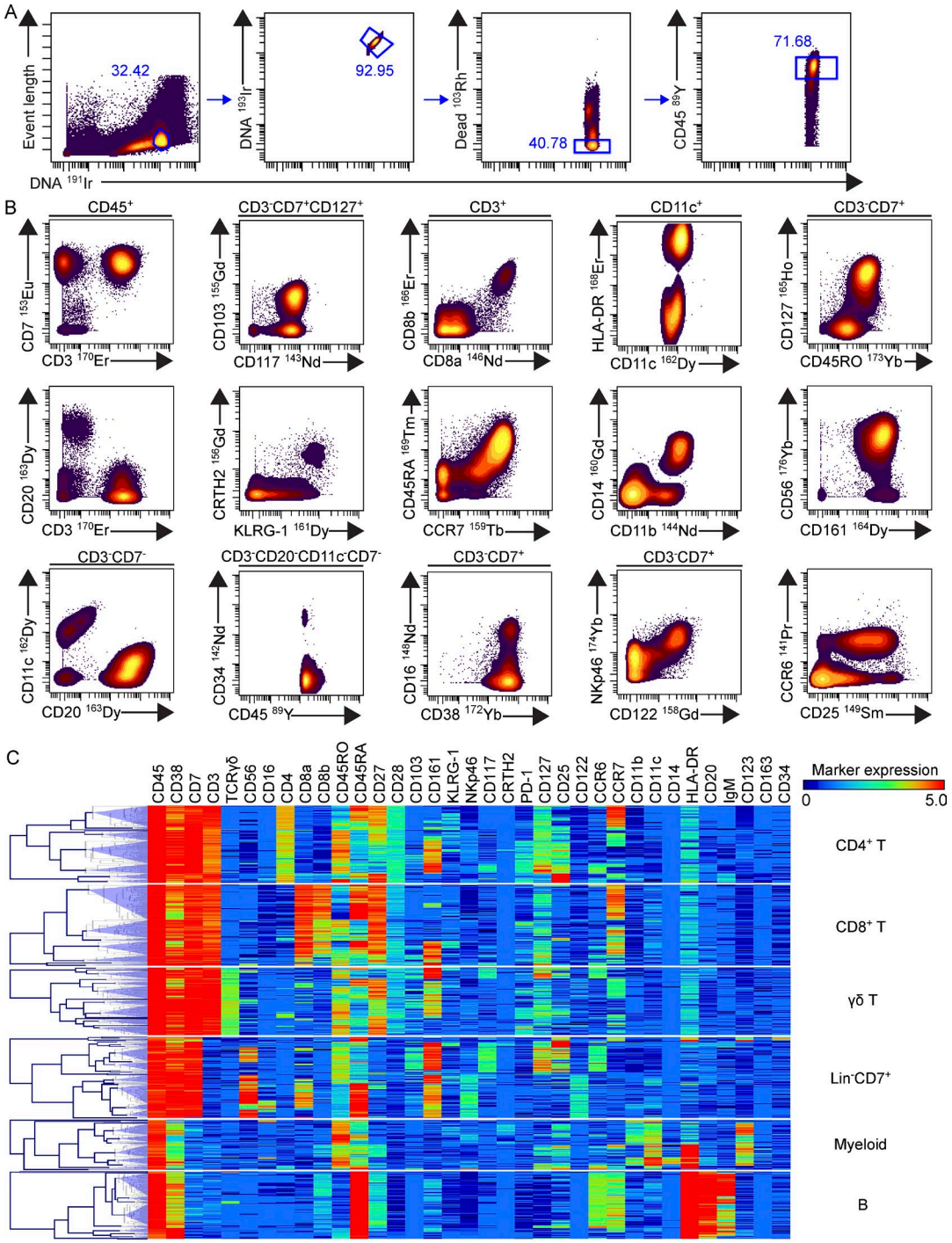

Figure S1. **Analysis of the entire immune system in the human fetal intestine using mass cytometry. (A)** Representative biaxial density dot plots from one fetal intestine showing the gating strategy for single, live CD45⁺ cells with percentages analyzed by mass cytometry (n = 7). Event length is a mass cytometry parameter defined as signal duration for the number of scans taken to acquire a given ion cloud. **(B)** Representative biaxial density dot plots from one fetal intestine showing the typical cell staining profiles of the antibodies used in mass cytometry after gating as shown in A (n = 7). Gated cell populations are annotated above the plots. **(C)** A heat map showing the median ArcSinh5-transformed marker expression values of the total 907 clusters identified by analyzing the entire immune system (CD45⁺ cells) from seven fetal intestines using the t-SNE–ACCENSE analysis pipeline (clustering per individual sample) for each of the six major immune lineages individually, as described before (van Unen et al., 2016), and hierarchical clustering thereof.

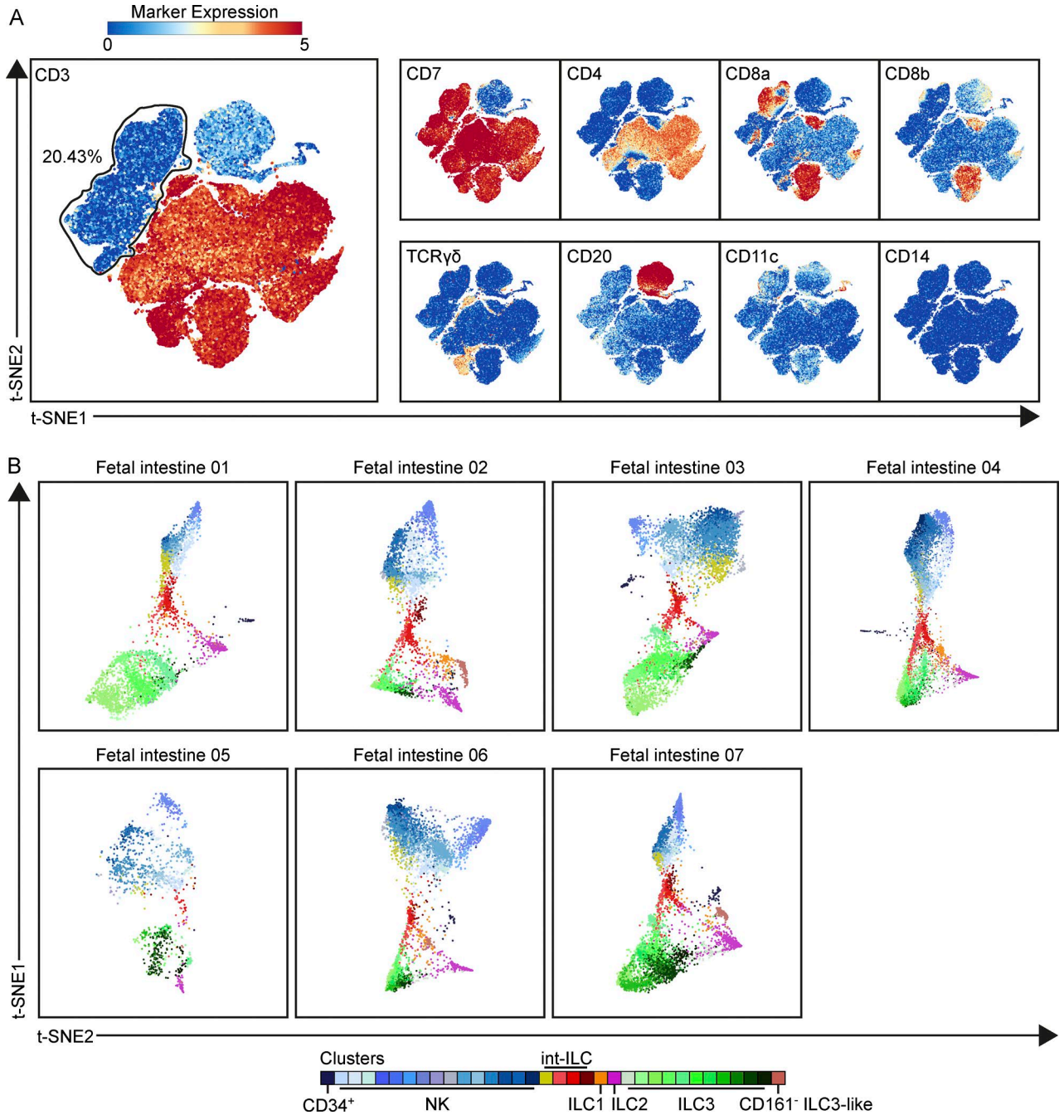

Figure S2. **t-SNE–based analysis of the Lin⁻CD7⁺ innate immune compartment in the human fetal intestine. (A)** Gating strategy of the Lin⁻CD7⁺ innate cell population in the human fetal intestine. t-SNE embeddings of the collective CD45⁺ cells (2.2×10^5 cells) from seven fetal intestines at single-cell resolution. Colors of cells represent ArcSinh5-transformed expression values of indicated markers. **(B)** Monitoring t-SNE computation dynamics for each individual fetal intestine. t-SNE embeddings of the ILC mass cytometry data showing single cells at stage 4 of the optimization course of the t-SNE computation for each individual fetal intestine ($n = 7$). Colors represent the cluster partitions.

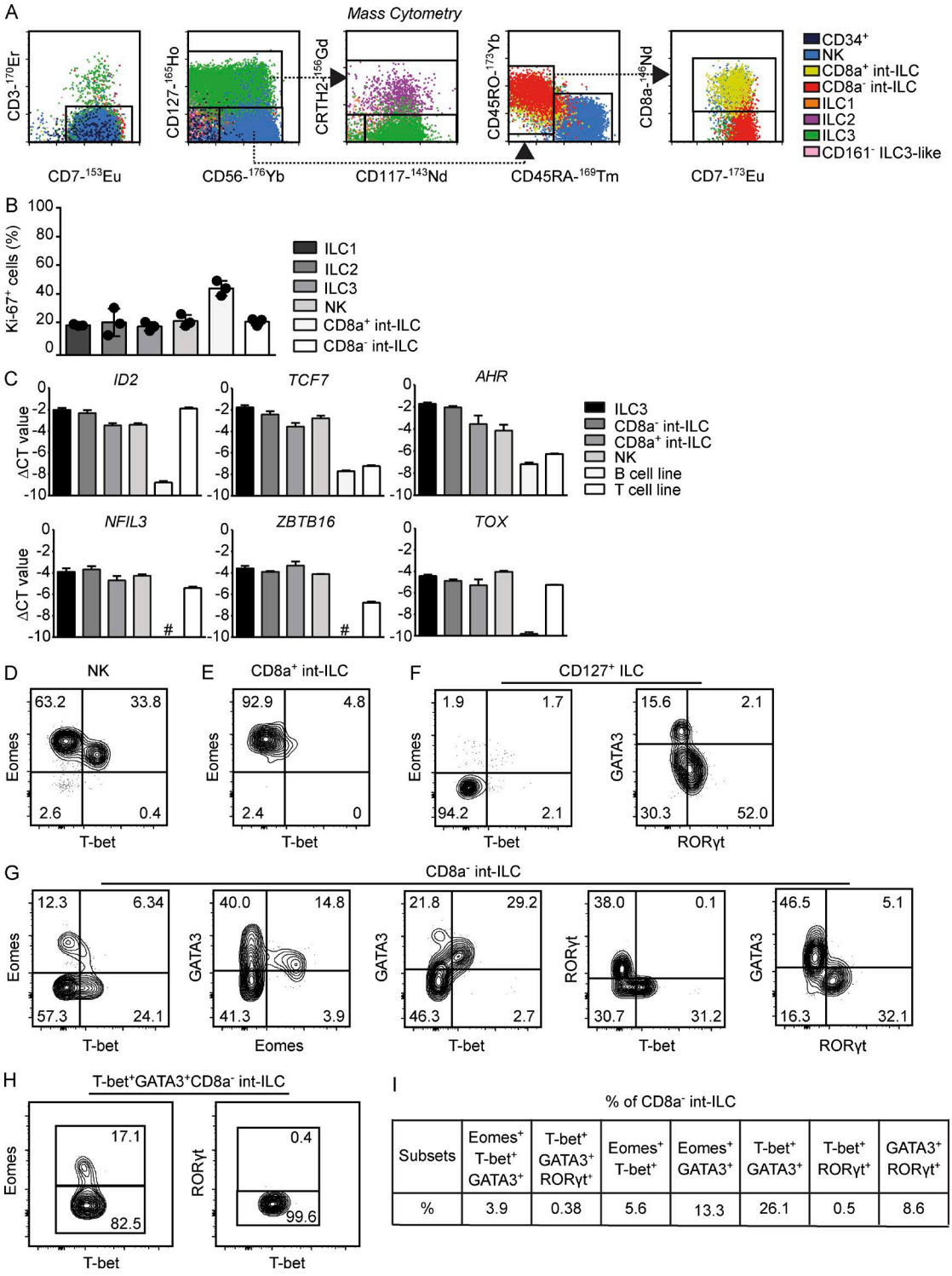

Subsets	Eomes+ T-bet+ GATA3+	T-bet+ GATA3+ RORγt+	Eomes+ T-bet+	Eomes+ GATA3+	T-bet+ GATA3+	T-bet+ RORγt+	GATA3+ RORγt+
%	3.9	0.38	5.6	13.3	26.1	0.5	8.6

Figure S3. **Ki-67 and transcription factor expression profiles of fetal intestinal ILCs ex vivo. (A)** Minimal antibody panel required for phenotyping ILC and int-ILC subsets in the human fetal intestine. Biaxial plots showing the expression of the indicated markers by ILC1, ILC2, ILC3, NK, and int-ILC subsets based on mass cytometry data derived from seven human fetal intestines. Color represents the different subsets identified by the t-SNE–based analysis shown in Fig. 1 B, and numbers of x-axis and y-axis represent ArcSinh5-transformed expression values of indicated markers. **(B)** Quantification of Ki-67–positive cells within indicated subsets obtained from three different human fetal intestines (two independent experiments). Error bar shows mean ± SD. **(C)** Relative mRNA expression of *ID2*, *TCF*, *AHR*, *NFIL3*, *ZBTB16*, and *TOX* by the purified ILC subsets. B- and T-cell lines analyzed by real-time PCR (three independent experiments). *GAPDH* as reference gene. #, The ΔCt value is below −10. Error bar shows mean ± SD. **(D)** Representative biaxial plots showing the expression of T-bet and Eomes, and GATA3 and RORγt by fetal intestinal CD127+ ILC. **(E and F)** Representative biaxial plots showing the expression of T-bet and Eomes by (E) fetal intestinal NK cells, and (F) CD8a+ int-ILC as defined in Fig. 3 A with flow cytometry. **(G)** Representative biaxial plots showing the combinatorial expression profiles of Eomes, T-bet, GATA3, and RORγt by fetal intestinal CD8a− int-ILC. **(H)** Expression of Eomes and RORγt by fetal intestinal T-bet+GATA3+CD8a− int-ILC. **(I)** Quantification of transcription factor positive cells of fetal intestinal CD8a− int-ILC (two independent experiments).

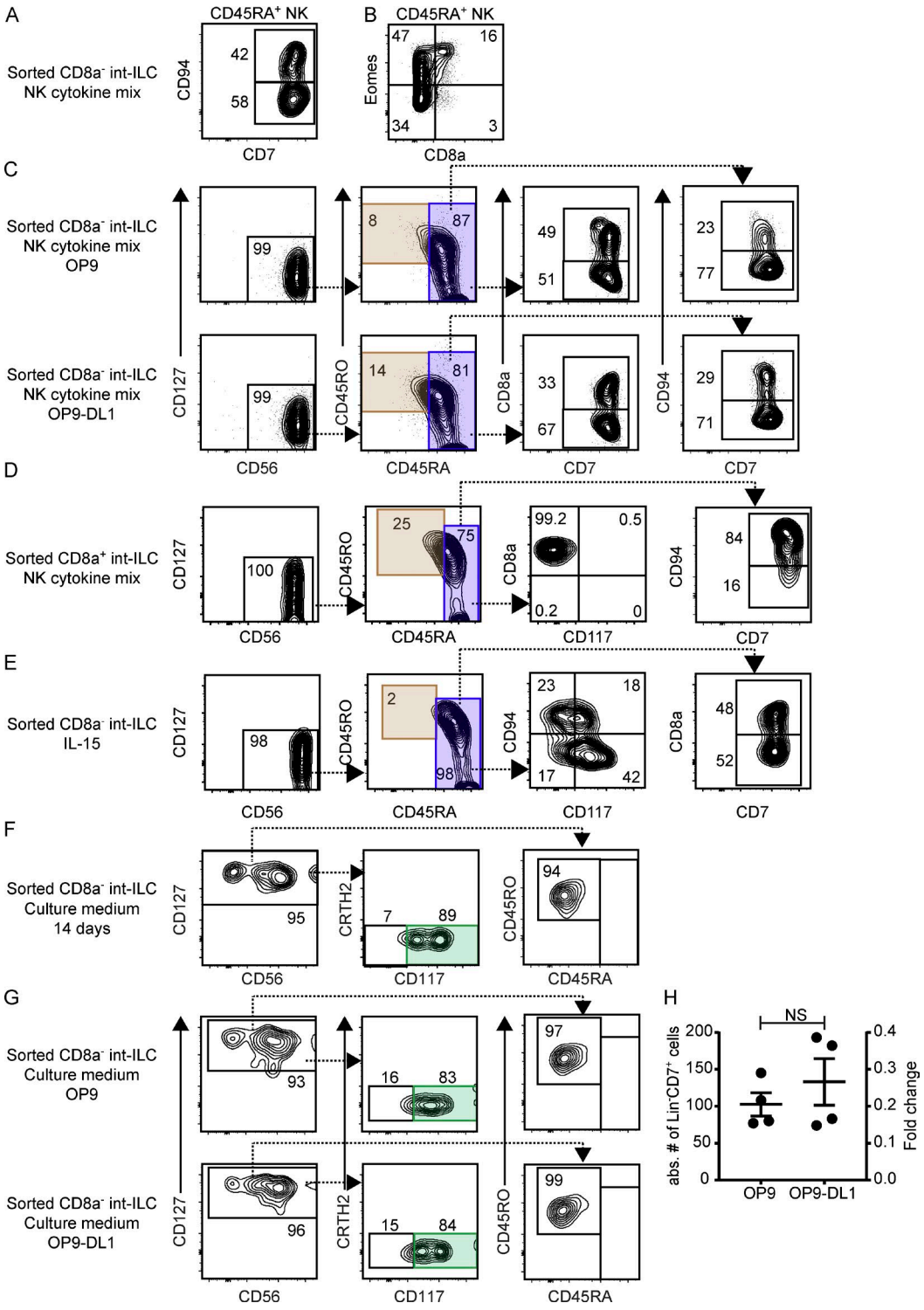

Figure S4. **CD8a⁻ int-ILC can differentiate into CD45RA⁺ NK cells and ILC3. (A–E)** Purified CD8a⁻ int-ILC (500 cells/well) and CD8a⁺ int-ILC (100 cells/well) populations were cocultured with irradiated OP9-DL1 or OP9 stromal cells for 7 d either with culture medium supplemented with either NK cytokine mix or IL-15. Generated cells were harvested and analyzed by flow cytometry. Duplicated wells were included for each condition in each experiment. Representative plots show a single duplicate. Biaxial plots show the expression of CD94 (A) and the transcription factor Eomes (B) by generated CD45RA⁺ NK cells from sorted CD8a⁻ int-ILCs with NK cytokine mix (three to five independent experiments). Representative biaxial plots depict the phenotypes of the generated Lin⁻CD7⁺ cells from sorted CD8a⁻ int-ILCs with NK cytokine mix with irradiated OP9-DL1 or OP9 stromal cells (C), sorted CD8a⁺ int-ILCs with NK cytokine mix (D), and sorted CD8a⁻ int-ILCs with IL-15 (E; two independent experiments). **(F–H)** Purified CD8a⁻ int-ILC (500 cells/well) were cocultured either with irradiated OP9-DL1 or with OP9 stromal cells with cytokine-free culture medium for 14 d (F) and 7 d (G and H). Generated cells were harvested and analyzed by flow cytometry (F and G). Representative biaxial plots depict the phenotypes of the generated Lin⁻CD7⁺ cells (two independent experiments). (H) Quantification of the generated Lin⁻CD7⁺ cells in absolute cell number (left axis) and fold change (right axis) compared with the number of initially sorted cells (two independent experiments). Error bar shows mean ± SEM. Statistical significance was determined with Student's *t* test by Prism GraphPad software.

Table S1, included as an Excel file, lists the information of antibodies used in the mass cytometry data.

Reference

van Unen, V., N. Li, I. Molendijk, M. Temurhan, T. Höllt, A.E. van der Meulen-de Jong, H.W. Verspaget, M.L. Mearin, C.J. Mulder, J. van Bergen, et al. 2016. Mass Cytometry of the Human Mucosal Immune System Identifies Tissue- and Disease-Associated Immune Subsets. *Immunity.* 44:1227–1239. https://doi.org/10.1016/j.immuni.2016.04.014